International Journal of Pharmaceutics 393 (2010) 268–272

Contents lists available at ScienceDirect

International Journal of Pharmaceutics

journal homepage: www.elsevier.com/locate/ijpharm

Pharmaceutical Nanotechnology

N-(2-hydroxyl) propyl-3-trimethyl ammonium chitosan chloride nanoparticle as a novel delivery system for Parathyroid Hormone-Related Protein 1–34

Sheng-hao Zhao[a], Xiao-ting Wu[b], Wei-chun Guo[a,*], Yu-min Du[b], Ling Yu[a], Jin Tang[a]

[a] Department of Orthopedics, Renmin Hospital of Wuhan University, Wuhan 430060, China
[b] Department of Environmental Science, College of Resource and Environmental Science, Wuhan University, Wuhan 430097, China

ARTICLE INFO

Article history:
Received 13 March 2010
Received in revised form 13 April 2010
Accepted 26 April 2010
Available online 8 May 2010

Keywords:
PTHrP1–34
Chitosan
EPTAC
HTCC
Nanoparticles

ABSTRACT

Chitosan (CS) and epoxy propyl trimethyl ammonium chloride (EPTAC) were used to prepare the water-soluble N-(2-hydroxyl) propyl-3-trimethyl ammonium chitosan chloride (HTCC). HTCC and sodium tripolyphosphate (TPP) were mixed to form HTCC nanoparticles based on ionic gelation. Parathyroid Hormone-Related Protein 1–34 (PTHrP1–34) was incorporated into the HTCC nanoparticles. The particle size and morphology of nanoparticles were determined by transmission electron microscopy (TEM). HTCC/PTHrP1–34 nanoparticles were 100–180 nm in size and their encapsulation efficiency and loading capacity were related to HTCC concentration, TPP concentration and initial concentration of PTHrP1–34. Relatively optimum encapsulation efficiency (78.4%) and loading capacity (13.7%) of PTHrP1–34 is achieved, and the in vitro release profile of PTHrP1–34 from nanoparticles has an initial burst, which is followed up by a slow release phase. These studies showed that HTCC/PTHrP1–34 nanoparticles are suitable for the treatment of osteoporosis, because of their slow-continuous-release properties, and the relevant in vivo experiments and clinical trials should be further studied.

1. Introduction

Natural polymers, especially polysaccharide nanoparticles have been widely investigated as a carrier for drug delivery (Gref et al., 1994; Kompella and Lee, 2001; Douglas et al., 2006; Krauland and Alonso, 2007). Nanoparticulate systems have attracted particular interests for the following reasons. Firstly, they can protect drugs from degradation (Lowe and Temple, 1994). Secondly, they improve drug transmucosal transport (Janes et al., 2001) and transcytosis by M cells (Clark et al., 2001). Thirdly, they can provide controlled release properties for encapsulated drugs (Galindo-Rodriguez et al., 2005).

Chitosan (CS) is the second most abundant polysaccharide found on earth next to cellulose. Because of its favorable biological properties such as biocompatibility, biodegradability, nontoxicity and antimicrobial activity (Hejazi and Amiji, 2003), CS has been widely used in pharmaceutical, medical areas, extensively researched as a primary material in forming carriers for therapeutic protein molecules and as non-viral gene carrying vectors (Douglas et al., 2006; George and Abraham, 2006; Dang and Leong, 2006). However, this activity is limited to acidic conditions due to its poor solubility above pH 6.5, where chitosan starts to lose its cationic nature (Liu et al., 2001). N-(2-hydroxyl) propyl-3-trimethyl ammonium chitosan chloride (HTCC) that can be prepared by a relatively easy chemical reaction of CS and epoxy propyl trimethyl ammonium chloride (EPTAC) has been reported (Lang et al., 1990; Lim and Hudson, 2004). HTCC has excellent water solubility over wide pH range, for its original amino group replaced by methyl, which prevented the generation of hydrogen bonds by chitosan amino and hydroxyl groups, so that HTCC can be dissolved in neutral and alkaline conditions (Lim and Hudson, 2004; Jia et al., 2001). Besides, HTCC has the potential to be used as an absorption enhancer across intestinal epithelial due to its mucoadhesive and permeability enhancing property (Kotzé et al., 1999; Li et al., 2007). HTCC nanoparticles have been formed based on ionic gelation process of HTCC and sodium tripolyphosphate (TPP). It has been reported that bovine serum albumin (BSA) can be incorporated into the HTCC nanoparticles, forming a novel BSA–HTCC nanoparticles, from which BSA can release slowly and continuously (Xu et al., 2003).

Parathyroid Hormone-Related Protein (PTHrP) was initially found to be a polypeptide in a research of malignacy induced hypercalcinemia, and it can effectively enhance the bone formation (Philbrick et al., 1996). A recent study showed that PTHrP can promote the proliferation of osteoblast and immature bone-like cells (Chen et al., 2004). An in vivo study also confirmed that different fragments of PTHrP (PTHrP1–34, 1–36, 1–74) can significantly

* Corresponding author at: Department of Orthopedics, Renmin Hospital of Wuhan University, 238 Jiefang Road, Wuhan 430060, China.
Tel.: +86 27 8804 1919x2209; fax: +86 27 8804 2292.
E-mail address: guoweichun@hotmail.com (W.-c. Guo).

0378-5173/$ – see front matter © 2010 Elsevier B.V. All rights reserved.
doi:10.1016/j.ijpharm.2010.04.034

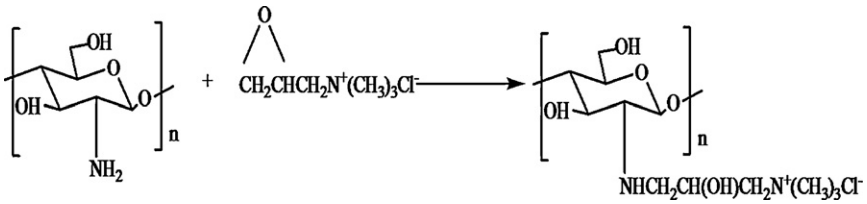

Scheme 1. Synthesis scheme of HTCC.

change bone mass and the biomechanic strength of the bone in osteoporosis rat (Stewart et al., 2000). It was reported that low dose and intermittent administration of PTHrP1–34 has a state effect on post-menopause osteoporosis women (Horwitz et al., 2003). Nevertheless, it has many shortcomings such as it gets denatured easily at normal temperature and it is very expensive which limit its use. Therefore, it is necessary to prepare a delayed release system to improve PTHrP1–34 bioactivity and a constant release. Nanoparticulate systems would be a better choice.

This research has prepared a new delayed release system for PTHrP1–34, and evaluated their in vitro releasing characteristics.

2. Materials and methods

2.1. Materials

CS was purchased from Yuhuan Ocean Biochemical Co. (Zhejiang Taizhou, China), deacetylation degree was 92%, and molecular weight (Mw) was 210,000. EPTAC was purchased from Dongying Guofeng Fine Chemical Co. (Shandong Dongying, China). TPP was purchased from Sinopharm Chemical Reagent Beijing Co. (Beijing, China). PTHrP1–34 was purchased from Sigma–Aldrich (Missouri, USA). All other chemicals were of reagent grade.

2.2. Preparation of HTCC

The HTCC was prepared in a similar manner to the method reported by Lim and Hudson (2004) (Scheme 1). Chitosan was dissolved in 2% (w/v) acetic aqueous solution. 15% (w/v) sodium hydroxide solution was added dropwise into the solution until pH reach 8–9. Chitosan precipitation was put into flask, as well as isopropanol, stirring the mixture until the chitosan was evenly dispersed, heating the solution to 80 °C. EPTAC was added dropwise into solution, with sufficient reaction for 6 h. The product was precipitated using acetone, washed repeatedly until the solution become neutral, dissolved in distilled water. The end-product was obtained by freeze drying after 5-day dialysis. The HTCC product's yield rate was about 30%, quaternization degree was 0.85 and the molecular weight was 1.08×10^5.

2.3. Preparation of HTCC nanoparticles and HTCC/PTHrP1–34 nanoparticles

HTCC was dissolved in distilled water at various concentrations (0.5, 1.0, 1.5, 2.0, and 2.5 mg/ml), and then while stirring at room temperature, 2 ml TPP aqueous solution with various concentrations (0.4, 0.6, 0.8, and 1.0 mg/ml) was added to 5 ml of HTCC solution. Three kinds of formations were observed: solution, aggregates and opalescent suspension. The zone of opalescent suspension was further examined by TEM as nanoparticles.

HTCC/PTHrP1–34 nanoparticles were formed spontaneously upon incorporation of 2 ml of the TPP solution (0.6 and 0.8 mg/ml) and 5 ml of the HTCC solution containing various concentrations of PTHrP1–34 (10, 30, 40, 80,120, and 160 μg/ml), with the conditions of stirring at room temperature for 2 h. Encapsulation efficiency of the different formations was determined by ultra-centrifugation of samples at 20,000 × g and 4 °C for 30 min. Thus the amount of free PTHrP1–34 was in clear supernatant determined by ELISA with PTHrP1–34 Kit (purchased from Groundwork Biotechnology Diagnosticate Ltd., CA, USA). The precipitates separated from suspension were dried by a freeze dryer. The PTHrP1–34 encapsulation efficiency (AE) and the PTHrP1–34 loading capacity (LC) of the nanoparticles were calculated as follows:

$$\mathrm{AE} = \frac{A - B}{A} \times 100$$

$$\mathrm{LC} = \frac{A - B}{N} \times 100$$

where A is the total amount of PTHrP1–34; B is the free amount of PTHrP1–34; and N is the amount of nanoparticles weight. All measurements were performed in triplicate.

2.4. Physicochemical characterization of nanoparticles

^{13}C NMR spectrum of sample in D_2O was recorded on a Varian Mercury 300 Spectrometer. IR spectra of CS, HTCC, HTCC nanoparticles, HTCC/PTHrP1–34 nanoparticles and PTHrP1–34 were taken with KBr pellets on PerkinElmer spectrum on FTIR. The particle size and morphological measurements of the nanoparticles were performed by TEM-100CXII.

2.5. Ammonium glycyrrhizinate releasing from the nanoparticles in vitro

In vitro PTHrP1–34 release profiles of HTCC/PTHrP1–34 nanoparticles were determined as follows. The PTHrP1–34-loaded HTCC nanoparticles separated from suspension were placed into test tubes with 10 ml 0.2 mol/L PBS solution (pH 7.4) and incubated at 37 °C while stirring. At appropriate time intervals, samples were ultracentrifuged at 20,000 × g and 4 °C for 30 min 2 ml of the supernatant was removed and 2 ml fresh medium PBS solution was added into the system. The amount of PTHrP1–34 in the release medium was evaluated by ELISA with PTHrP1–34 Kit. The calibration curve was made using non-loaded PTHrP1–34 nanoparticles. All release tests were run in triplicate and the mean value was reported.

3. Results and discussion

3.1. Physicochemical characterization of HTCC and nanoparticles

Fig. 1 shows FTIR spectra of CS, HTCC, HTCC nanoparticles, HTCC/PTHrP1–34 nanoparticles and PTHrP1–34. There are three characteristic peaks of CS at 3441 cm^{-1} of υ(OH), 1600 cm^{-1} of $\upsilon(NH_2)$ and 1061 cm^{-1} of δ(C–O–C) (Yu et al., 1999). Compared with CS, HTCC shows the disappearance of the NH_2-associated band at 1600 cm^{-1} of the N–H bending in the primary amine; and appearance of a new band at 1480 cm^{-1}, which is attributed to the methyl groups of the ammonium (Suzuki et al., 2000; Qin et al., 2002).

The spectrum of HTCC nanoparticles (Fig. 1(1)) is different from that of HTCC matrix (Fig. 1(2)). In HTCC nanoparticles the

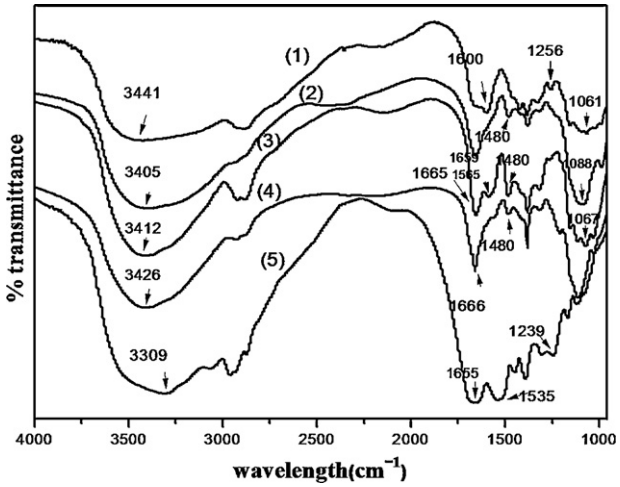

Fig. 1. FTIR of CS (1), HTCC (2), HTCC nanoparticles (3), HTCC/PTHrP1–34 nanoparticles (4) and PTHrP1–34 (5).

intensity of 1480 cm^{-1} peak becomes weaker, 1659 cm^{-1} shifts to 1669 cm^{-1}, and a new peak of 1565 cm^{-1} appears. We suppose that TPP was linked with ammonium groups of HTCC in nanoparticles. The IR spectrum is consistent with the reported spectra (Knaul et al., 1999). Hydroxyl group absorption of CS at 1256 cm^{-1} almost disappears in HTCC nanoparticles, which indicates that free hydroxyl groups form hydrogen bonding. Acetylamino υ(NH2) I 1655 cm^{-1}, II 1535 cm^{-1} and III 1239 cm^{-1}, respectively are the characteristic peaks of PTHrP1–34. Acetylamino I 1655 cm^{-1} in PTHrP1–34 overlaps with δ(NH) 1665 cm^{-1} in HTCC nanoparticles, so the peak of 1666 cm^{-1} in HTCC/PTHrP1–34 nanoparticles is more intensive than that in PTHrP1–34.

The ^{13}C NMR spectrum of HTCC was illustrated in Fig. 2. There is a significant absorption peak when δ = 54.325 ppm, which corresponded to the three methyliums C_4^* of side chain on HTCC, and it was the maximum absorption peak. The peak of δ = 101.1, 64.9, 73.2, 74.9 and 77.6 ppm demonstrated C_1, C_2, C_3, C_4 and C_5 from heterocycle respectively. The peak of δ = 53.6, 65.4 and 69.3 ppm represented the C_1^*, C_2^* and C_3^* from the side chain of HTCC. This provided the evidence that there was an EPTAC substitution reaction on the C_2 site of chitosan.

3.2. Morphological characteristic of nanoparticles

Fig. 3 shows the morphological characteristic of nanoparticles. HTCC nanoparticles (Fig. 3A) and HTCC/PTHrP1–34 nanoparticles

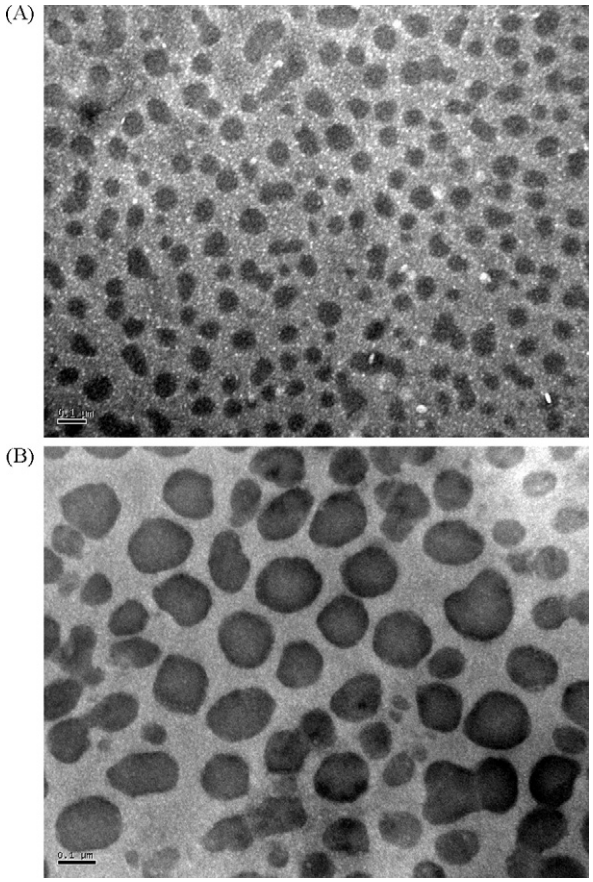

Fig. 3. TEM of HTCC nanoparticles (60k)(A) and the PTHrP1–34-loaded nanoparticles (80k) (B) (HTCC 1.5 mg/ml, TPP 0.6 mg/ml, PTHrP1–34 120 μg/ml).

(Fig. 3B) take spherical shape and are monodisperse. HTCC nanoparticles are about 90–100 nm while HTCC/PTHrP1–34 nanoparticles are about 100–180 nm. PTHrP1–34 loading significantly increased nanoparticles size in comparison to HTCC nanoparticles, possibly due to the surface absorption of PTHrP1–34 that has large molecular weight and size.

3.3. Encapsulation efficiency of PTHrP1–34-loaded nanoparticles

Fig. 4 shows that encapsulation efficiency and loading capacity of the nanoparticles were affected by the initial PTHrP1–34

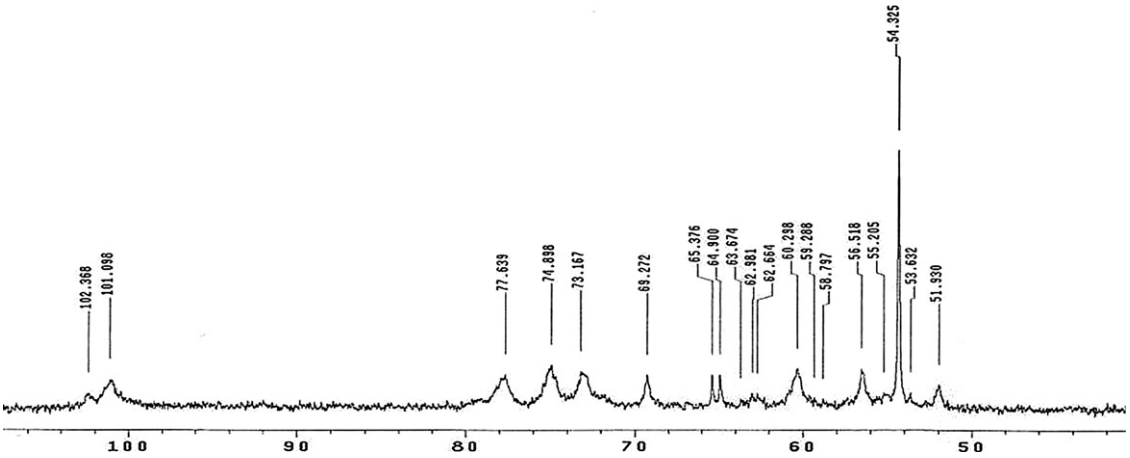

Fig. 2. The ^{13}C NMR spectrum of HTCC in D_2O.

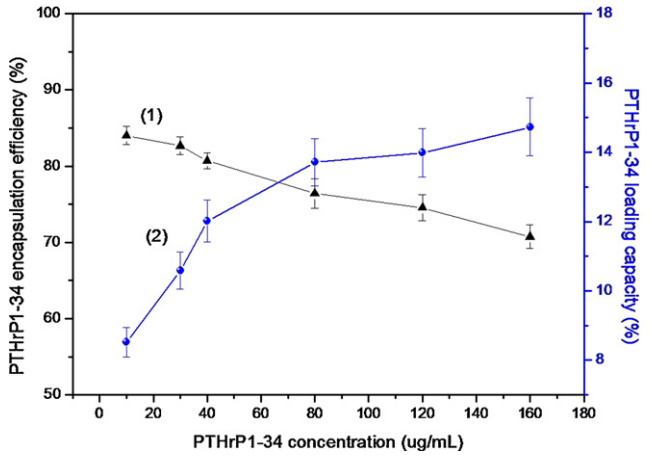

Fig. 4. PTHrP1–34 encapsulation efficiency (1) and PTHrP1–34 loading capacity (2) of HTCC nanoparticles (HTCC 1.5 mg/ml, TPP 0.6 mg/ml). All data are the mean ± standard deviation ($n = 4$).

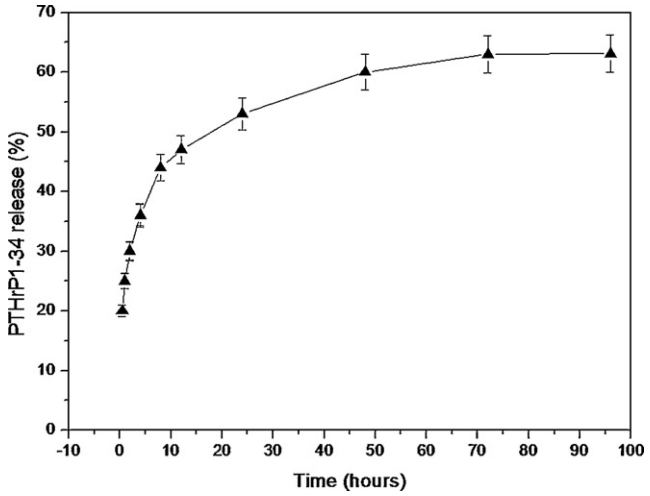

Fig. 6. PTHrP1–34 release profile from PTHrP1–34-loaded HTCC nanoparticles (HTCC 1.5 mg/ml, TPP 0.6 mg/ml, PTHrP1–34 160 μg/ml).

concentration. As for preparation with TPP 0.6 mg/ml, increasing PTHrP1–34 concentration from 10 to 160 μg/ml decreased encapsulation efficiency of PTHrP1–34 from 84% to 70% (Fig. 4(1)) and increased loading capacity of PTHrP1–34 from 8.5% to 16.7% (Fig. 4(2)). Taking into account the extremely high price of PTHrP1–34, we tend to choose the initial PTHrP1–34 concentration 80 μg/ml with the encapsulation efficiency 78.4% and loading capacity 13.7%.

Fig. 5 shows the effect of HTCC concentration on encapsulation efficiency of PTHrP1–34. As for preparation with TPP 0.6 mg/ml, increasing HTCC concentration from 0.5 to 1.5 mg/ml increased encapsulation efficiency from 58.5% to 82.3%, and when continues to increase HTCC concentration to 2.0 mg/ml, the encapsulation efficiency decreases to 73.6% (Fig. 5(1)). As for preparation with TPP 0.8 mg/ml, increasing HTCC concentration from 1.5 to 2.5 mg/ml decreased encapsulation efficiency from 78.4% to 65.3% (Fig. 5(2)).

The ratio among HTCC, TPP, and PTHrP1–34 plays an important role in the formation of nanoparticles. Nanoparticles can format when the dosage of HTCC and the TPP is about 5:1 to 2:1. Too high HTCC concentration (2.0–2.5 mg/ml) led to clear solution, no nanoparticles formation, too high TPP (1.2 mg/ml) led to aggregates with large size. Loading capacity of PTHrP1–34 increased by increasing the initial PTHrP1–34 concentration in HTCC solution, meanwhile, the encapsulation efficiency of PTHrP1–34 decreased.

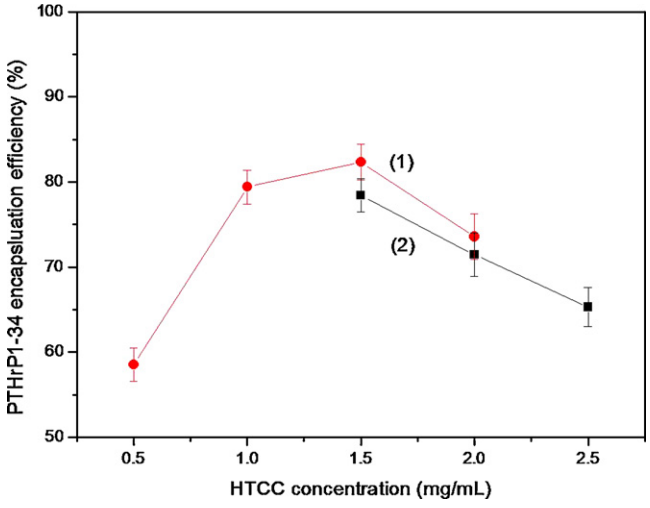

Fig. 5. The influence of HTCC concentration on PTHrP1–34 encapsulation efficiency ((1) TPP 0.6 mg/ml, PTHrP1–34 40 μg/ml; (2) TPP 0.8 mg/ml, PTHrP1–34 40 μg/ml). All data are the mean ± standard deviation ($n = 4$).

3.4. *In vitro release of PTHrP1–34 from HTCC/PTHrP1–34 nanoparticles*

Fig. 6 displayed the release profile of PTHrP1–34 from nanoparticles. It was apparent that PTHrP1–34 release in vitro showed a very rapid within initial 8 h, and then followed by a very slow drug release after about 10 h. After 3 days, around 60% of drugs typically release from nanoparticles, but no more drugs release after 4 days, indicating part of the PTHrP1–34 is not completely released. The consensus understanding of protein release from chitosan particulate systems involves three different mechanisms (Xu et al., 2003). (a) The first burst release of 21–45%, due to the drug desorption from the particles surface, which easily diffuse in the initial incubation time. (b) A reversed release in following about 4 h, due to PTHrP1–34 readsorption onto nanoparticles surface again. HTCC nanoparticles swelled immediately in PBS in Fig. 3, the increased specificity of particles may lead to a high amount of PTHrP1–34 readsorption. This phenomenon has also been observed in previous reports (Bouillot et al., 1999; Zambaux et al., 2001). (c) A constant sustained release of the drug for the following 3 days, resulting from the diffusion of the drug dispersed in the polymer matrix and then through the polymer wall as well as its erosion.

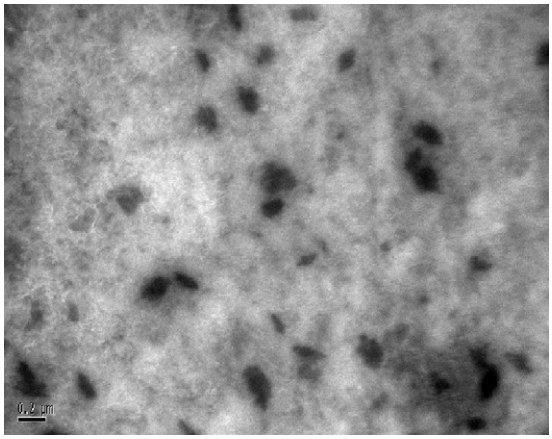

Fig. 7. TEM of PTHrP1–34-loaded nanoparticles which have been placed in PBS solution for 48 hours (40k) (HTCC 1.5 mg/ml, TPP 0.6 mg/ml, PTHrP1–34 80 μg/ml).

As shown in Fig. 7, morphological characteristic of PTHrP1–34-loaded nanoparticles has mostly changed to irregular shape after 2 days. Particles diameter reduced to varying degrees, and some particles were of serious corrosion as the polymer depolymerization possibly.

4. Conclusion

This study demonstrates that water-soluble HTCC which was prepared by a relatively easy chemical reaction of CS and EPTAC can form nanoparticles based on ionic gelation process with TPP. HTCC nanoparticles had shown an excellent capacity for the association of PTHrP1–34, and formed spherical and monodispersed particles with a mean diameter of 100–180 nm by an ionic gelation method at room temperature and neutral environment. Relatively optimum encapsulation efficiency (78.4%) and loading capacity (13.7%) of PTHrP1–34 is achieved, and the release profile of PTHrP1–34 from nanoparticles has a burst and a slowly continuous release phase followed. The HTCC/PTHrP1–34 nanoparticles may be provided for in vivo application of anti-osteoporosis, the relevant in vivo experiments and clinical trials to be further studied.

Acknowledgements

The authors thank professor Du (Wuhan University, Wuhan, China) for his helpful suggestions. This work was supported by the Scientific and Technological project of Hubei Province of China (No. 2007AA402C89) and Planning Project of Innovative Experiment of National Undergraduate (No. 081048645).

References

Bouillot, P., Ubrich, N., Sommer, F., Duc, T.M., Loeffler, J.P., Dellacherie, E., 1999. Protein encapsulation in biodegradable amphiphilic microspheres. Int. J. Pharm. 181, 159–172.

Chen, C., Koh, A.J., Datta, N.S., Zhang, J., Keller, E.T., Xiao, G., Franceschi, R.T., D'Silva, N.J., McCauley, L.K., 2004. Impact of the mitogen activated protein kinase pathway on parathyroid hormone-related protein actions in osteoblasts. J. Biol. Chem. 279, 29121–29129.

Clark, M.A., Blair, H., Liang, L., Brey, R.N., Brayden, D., Hirst, B.H., 2001. Targeting polymerised liposome vaccine carriers to intestinal M cells. Vaccine 20, 208–217.

Dang, J.M., Leong, K.W., 2006. Natural polymers for gene delivery and tissue engineering. Adv. Drug. Deliv. Rev. 58, 487–499.

Douglas, K.L., Piccirillo, C.A., Tabrizian, M., 2006. Effects of alginate inclusion on the vector properties of chitosan-based nanoparticles. J. Control. Release 115, 354–361.

Galindo-Rodriguez, S.A., Allemann, E., Fessi, H., Doelker, E., 2005. Polymeric nanoparticles for oral delivery of drugs and vaccines: a critical evaluation of in vivo studies. Crit. Rev. Ther. Drug Carrier Syst. 22, 419–464.

George, M., Abraham, T.E., 2006. Polyionic hydrocolloids for the intestinal delivery of protein drugs: alginate and chitosan—a review. J. Control. Release 114, 1–14.

Gref, R., Minamitake, Y., Peracchia, M.T., Trubetskoy, V., Langer, R., 1994. Biodegradable long-circulating polymeric nanospheres. Science 236, 1600–1603.

Hejazi, R., Amiji, M., 2003. Chitosan-based gastrointestinal delivery systems. J. Control. Release 89, 151–165.

Horwitz, M.J., Tedesco, M.B., Gundberg, C., Garcia-Ocana, A., Stewart, A.F., 2003. Short-term, high-dose parathyroid hormone-related protein as a skeletal anabolic agent for the treatment of postmenopausal osteoporosis. J. Clin. Endocrinol. Metab. 88, 569–575.

Janes, K.A., Calvo, P., Alonso, M.J., 2001. Polysaccharide colloidal particles as delivery systems for macromolecules. Adv. Drug. Deliv. Rev. 47, 83–97.

Jia, Z., Shen, D., Xu, W., 2001. Synthesis and antibacterial of quaternary ammonium salt of chitosan. Carbohydr. Res. 333, 1–6.

Knaul, J.Z., Hudson, S.M., Creber, K.A.M., 1999. Improved mechanical properties of chitosan fibers. J. Appl. Polym. Sci. 72, 1721–1731.

Kompella, U.B., Lee, V.H., 2001. Delivery systems for penetration enhancement of peptide and protein drugs: design considerations. Adv. Drug Del. Rev. 46, 211–245.

Kotzé, A.F., Thanou, M.M., Luessen, H.L., de Boer, B.G., Verhoef, J.C., Junginger, H.E., 1999. Effect of the degree of quaternization of N-trimethyl chitosan chloride on the permeability of intestinal epithelial cells (Caco-2). Eur. J. Pharm. Biopharm. 47, 269–274.

Krauland, A.H., Alonso, M.J., 2007. Chitosan/cyclodextrin nanoparticles as macromolecular drug delivery system. Int. J. Pharm. 340, 134–142.

Lang, G., Wendel, H., Konard, E., 1990. Process for making quaternary chitosan derivatives for cosmetic agents. US Patent 4,921,949.

Li, T., Shi, X.W., Du, Y.M., Tang, Y.F., 2007. Quaternized chitosan/alginate nanoparticles for protein delivery. J. Biomed. Mater. Res. A. 83, 383–390.

Lim, S.H., Hudson, S.M., 2004. Synthesis and antimicrobial activity of a water-soluble chitosan derivative with a fiber-reactive group. Carbohydr. Res. 339, 313–319.

Liu, X.F., Guan, Y.L., Yang, D.Z., Li, Z., Yao, K.D., 2001. Antibacterial action of chitosan and carboxymethylated chitosan. J. Appl. Polym. Sci. 79, 1324–1335.

Lowe, P.J., Temple, C.S., 1994. Calcitonin and insulin in isobutylcyanoacrylate nanocapsules: protection against proteases and effect on intestinal absorption in rats. J. Pharm. Pharmacol. 46, 547–552.

Philbrick, W.M., Wysolmerski, J.J., Galbraith, S., Holt, E., Orloff, J.J., Yang, K.H., Vasavada, R.C., Weir, E.C., Broadus, A.E., Stewart, A.F., 1996. Defining the roles of parathyroid hormone-related protein in normal physiology. Physiol. Rev. 76, 127–173.

Qin, C.Q., Xiao, L., Du, Y.M., Shi, X.W., Chen, J.W., 2002. A new cross-linked quaternized-chitosan resin as the support of borohydride reducing agent. React. Funct. Polym. 50, 165–171.

Stewart, A.F., Cain, R.L., Burr, D.B., Jacob, D., Turner, C.H., Hock, J.M., 2000. Six-month daily administration of parathyroid hormone and parathyroid hormone-related protein peptides to adult ovariectomized rats markedly enhances bone mass and biomechanical properties: a comparison of human parathyroid hormone 1–34, parathyroid hormone-related protein 1–36, and SDZ-parathyroid hormone 893. J. Bone Miner. Res. 15, 1517–1525.

Suzuki, K., Shinobu, T., Saimoto, H., Shigemasa, Y., Oda, D., 2000. New selectively N-substituted quaternary ammonium chitosan derivatives. Polym. J. 32, 334–338.

Xu, Y., Du, Y., Huang, R., Gao, L., 2003. Preparation and modification of N-(2-hydroxyl) propyl-3-trimethyl ammonium chitosan chloride nanoparticle as a protein carrier. Biomaterials 24, 5015–5022.

Yu, J.H., Du, Y.M., Zheng, H., 1999. Blend films of chitosan-gelation. J. Wuhan Univ. (Nat. Sci. Ed.). 45, 440–444.

Zambaux, M.F., Bonneaux, F., Gref, R., Dellacherie, E., Vigneron, C., 2001. Protein C-loaded monomethoxypoly (ethylene oxide)-poly(lactic acid) nanoparticles. Int. J. Pharm. 212, 1–9.